



Calculation by Density functional theory of FeNi₂Mo and FeNi₂Nd

Faycal Baira ¹, Abderrahim Achouri ², Yamina Benkrima^{3,*}, Mohammed Elbar Soudani ⁴, Djamel Belfenache⁵, Radhia Yekhlef ^{5,6}, Samy Mansy⁷

¹ Department of Sciences and technology, Faculty of technology, University of Batna 2, Alleys 53, Constantine Avenue. Fésdis, Batna 05078, Algeria

² Université de Ouargla, Faculté des Mathématiques et des Sciences de la Matière, Lab. Développement des énergies nouvelles et renouvelables dans les zones arides et sahariennes, Ouargla 30000, Algeria

³Ecole normale supérieure de Ouargla, 30000 Ouargla, Algeria

⁴Laboratory for the Development of New and Renewable Energies in Arid and Saharan Zones, Faculty of Mathematics and Materials Science, Kasdi Merbah Ouargla University, Ouargla 30000 Algeria

⁵Research Center in Industrial Technologies CRTI, P.O. Box 64, Cheraga, 16014 Algiers, Algeria.

⁶Laboratory of Electrochemistry, Molecular Engineering and Redox Catalysis (LEIMCR) Department of Engineering Process, Faculty of Technology, Ferhat Abbas University Setif-1, Setif 19000, Algeria.

⁷University Collage of Science and Technology, Department of Engineering Science and Applied Arts, P.O. Box 8, KanYunis-Palestine.

1371

Received 10 March, 2023 Accepted 22 May, 2023 Published 13 July, 2023

Abstract:

Our calculations were done with the help of density functional theory (DFT) and use the generalized gradient approximation (GGA), The pseudo-potential linearised augmented plane wave (PP-LAPW) method is applied to solve the Kohn-Sham equations, in order to search for the structural, electronic and optical properties of the FeNi₃ original alloy, as well as the FeNi₂Mo and FeNi₂Nd alloys resulting from doping with (Mo, Nd) atoms in the original cell. The lattice parameters of the alloys were calculated and compared with previous theoretical and experimental results, the electronic properties such as energy bands and the total density of states showed the metallic property of the alloys and that the FeNi₂Nd alloy has more magnetic moment. Also it was found that the contribution of the 3-d orbital is dominant, and this appears by comparing the density of partial states recorded in the two alloys, and this affects the electronic and magnetic properties of the two alloys. The general results of optical properties including absorption coefficient, refractive index, optical conductivity of FeNi₂Mo and FeNi₂Nd are discussed and compared with each other, our results show new and important optical properties.

Keywords: DFT, Siesta, Alloys, Properties structural, Properties Optic.

DOI Number: 10.48047/nq.2023.21.6.NQ23139

NeuroQuantology2023;21(6): 1371-1378

1. INTRODUCTION

In recent years, nanomaterials have been revolutionizing the world as they offer new horizons in research and development, nanoparticles (NPs) are very small particles with lengths ranging from 1 to

100 nanometers, and they exist in many dimensions and at least one dimension, nanoparticles have a high surface area to volume ratio, thanks to which they can exhibit unique physical and chemical properties such as reactivity, versatility, and

*b-amina1@hotmail.fr



strength from their bulk counterparts [1-3]. Among these types of nanoparticles, interest in magnetic nanoparticles (MNPs) has been increasing due to their unique physical, chemical and magnetic properties [4-6]. These magnetic particles have many uses such as biomedicine [2], environmental remediation [1,5], catalysis [7], magnetic resonance imaging [8,9], data storage [10], and sensors [11], electromagnetic shielding [12], etc.

Iron-nickel alloys are an example of a metallic nanostructured magnetic alloy, which has received significant attention in recent years due to its desirable superiority in terms of magnetic and mechanical properties that make it applicable in many fields [13-15]. One of the most important features of Fe-Ni alloys is that we can prepare them in different sizes, shapes and compositions, depending on the method used in preparation [13]. Many researchers have been able to prepare a variety of morphological structures for iron-nickel alloys, including spherical particles [16], triangular particles [17], rods [18], platelets [19].

In this research paper, we will present a theoretical study on iron-nickel alloys doped with (Mo and Nd) atoms, and touch on an in-depth study on the structural, electronic and optical properties. This study is considered as the first theoretical study of this subject, which has not been addressed previously.

2. THEORETICAL APPROACH

FeNi₃ exists in face centered cube structure (fcc) and having lattice parameters, $a=b=c=3.548\text{Å}$, $\alpha = \beta = \gamma = 90.00^\circ$ (space group: Pm3m). On Mo-doping and Nd-doping, the lattice relaxation and movement of all the atoms were allowed to obtain the optimized structure using Spanish initiative for electronic Simulations with thousands of atoms (Siesta) [20], within generalized gradient approximation (GGA), based on density functional theory (DFT) [21], in basics with four atoms defined by the following reduced coordinates: Fe (0, 0, 0) and three enumerated for the convenience nickel atoms Ni₁ (1/2, 1/2, 0), Ni₂ (0, 1/2, 1/2), Ni₃ (1/2, 0, 1/2), where it was compared with the results of previous theoretical and experimental work. The unit cell in FeNi₂Mo and FeNi₂Nd were built by substituting a Mo and Nd atom in place of a Ni atom by successive relaxation. Using the conver-

gence criteria until the atomic forces were less than $5 \times 10^{-4} \text{eV/Å}$. For the calculation of electronic ground state properties of these alloys, we used spin polarization with Perdew-Burke-Ernzerhof (PBE) exchange-correlation functional within generalized gradient approximation (GGA). The Brillouin zone were sampled for these cells by a Monkhorst-Pack k-grid of $3 \times 3 \times 3$. The plane wave norm conserving pseudopotentials, created with the use of GGA-PBE approach, are obtained from library, with the valence electron coverage of Fe, Ni, Mo and Nd atoms are $3d^6 4s^2$, $3d^8 4s^2$, $4d^5 5s^1$ and $4f^4 6s^2$, correspondingly. The energy band structures are sketched along the k-path built on data taken from Hinuma statistics [24]. We represented the projected density of states along atomic valence orbitals (PDOS) in order to compare and reveal the role of electrons in different atomic valence orbitals, on electronic properties, especially on x-polarization. And from it, the spin polarization is determined due to the different distribution of spin states (spin up and spin down) and from it determine the magnetic moment of the unit cell. Besides the two fcc crystals of FeNi₃ as a pure crystal as a reference, some relevant calculation data of FeNi₂Mo alloy in comparison with FeNi₂Nd alloy are also represented for similarity of electronic properties.

3. RESULTS AND DISCUSSION

3.1. Alloys Structures

Structural parameters of an originally relaxed FeNi₃ cell with a Pm3m space group, formed by four atoms delimited by the following coordinates: Fe (0, 0, 0) and three relaxed Ni atoms Ni₁ (1/2, 1/2, 0), Ni₂ (0, 1/2, 1/2), Ni₃ (1/2, 0, 1/2). The lattice constants of FeNi₃ alloy over the past times have been verified many times, the primary structure of stable FeNi₃ alloy is the group structure of Pm3m and the lattice constants are estimated to be $a = b = c = 3.528 \text{Å}$, $\alpha = \beta = \gamma = 90.00^\circ$. Whereas in our present work, we find the lattice parameters for the new FeNi₂Mo alloy is $a = b = c = 3.532 \text{Å}$, while FeNi₂Nd alloy is $a = b = c = 3.592 \text{Å}$.

We based our calculations for this work on the Siesta code that was used to find the initial cell constants for FeNi₃, FeNi₂Mo and FeNi₂Nd alloys, this is done by replacing one of the nickel atoms with molybdenum (Mo) atom in the first time and neodymium (Nd) atom in the second time to obtain



FeNi₂Mo and FeNi₂Nd alloys. In this study, the results are compared with experiment data and previous theoretical work, and we present in Table 1 the structural parameters of the primary FeNi₃ cell, we obtained the lattice parameters of the cell FeNi₃, FeNi₂Mo and FeNi₂Nd (see Fig. 1).

Table 1. Structural parameters of the optimized FeNi₃, FeNi₂Mo and FeNi₂Nd alloys and compared with theoretical and experimental result.

	work	a (Å)	b (Å)	c (Å)
FeNi ₃	Our work	3.528	3.528	3.528
	Theor[22]	3.548	3.548	3.548
	Exep[23]	3.55	3.55	3.55
FeNi ₂ Mo	Our work	3.532	3.532	3.532
FeNi ₂ Nd	Our work	3.592	3.592	3.592

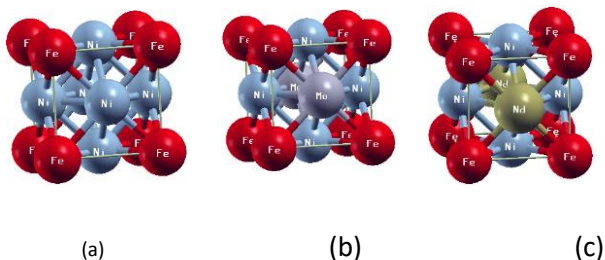


Fig. 1 – Structure of: (a) FeNi₃, (b) FeNi₂Mo, (c) FeNi₂Nd

It is observed from Table 1 that the obtained results are close to previous theoretical and experimental work, and that doping of the parent compound FeNi₃ with molybdenum (Mo) or neodymium (Nd) atoms changes the original cell dimensions and contributes to an increase in its volume.

3.2. Electronic Properties

3.2.1 Bands Structure

In order to study the basic structure, we choose a specific region called the Brillouin zone, in order to find the electronic properties of the material. Fig. 2 shows the Brillouin zone of the cubic structure. It is worth noting that the study of properties in this region can be generalized later on both FeNi₂Mo

and FeNi₂Nd alloys.

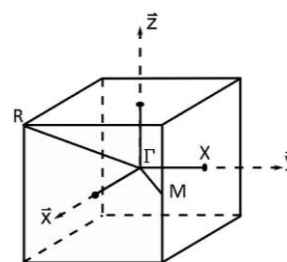


Fig. 2 – Brillouin zone of a cubic structure

In our study we used DFT theory and GGA approximation in order to determine the band gap of FeNi₂Mo and FeNi₂Nd alloys. This method has been relied upon because it is one of the most appropriate methods for studying the electronic structures of materials. Fig.3 shows the results of the structure of the energy bands for the alloys.

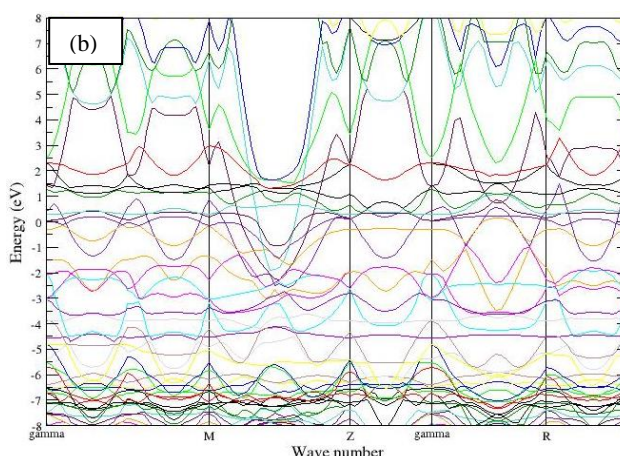
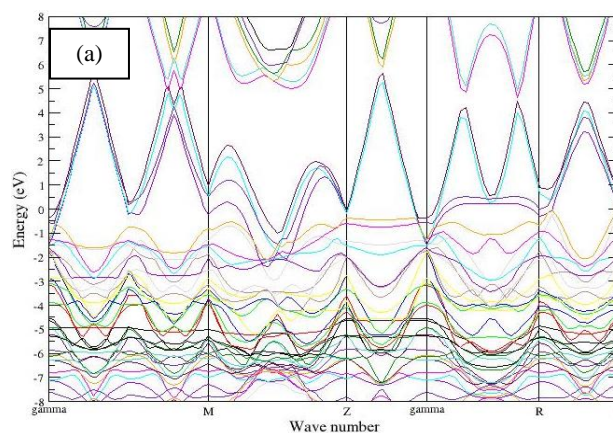


Fig. 3 – Energy bands structure of: (a) FeNi₂Mo,(b) FeNi₂Nd

As can be seen from Figs 3a and 3b, the highest valence bands overlap with the conduction bands, which is conclusive evidence of the metallicity of the two alloys,we also found that both alloys have ferromagnetic properties, with magnetic moments estimated to be 5.42 μ B and 5.53 μ B for FeNi₂Mo and FeNi₂Nd alloys respectively.

3.2.2. Electronic Density of States (DOS)

We plotted both the total density of states (TDOS) and the partial density of states (PDOS) for FeNi₂Mo and FeNi₂Nd alloys using the GGA approximation, and then analyzed them to determine the reason for the presence of states that formed valence and conductive-bands, and to understand the nature of interactions between the atoms of the studied alloys, as is Shown in Fig. 4 and Fig. 5 respectively.

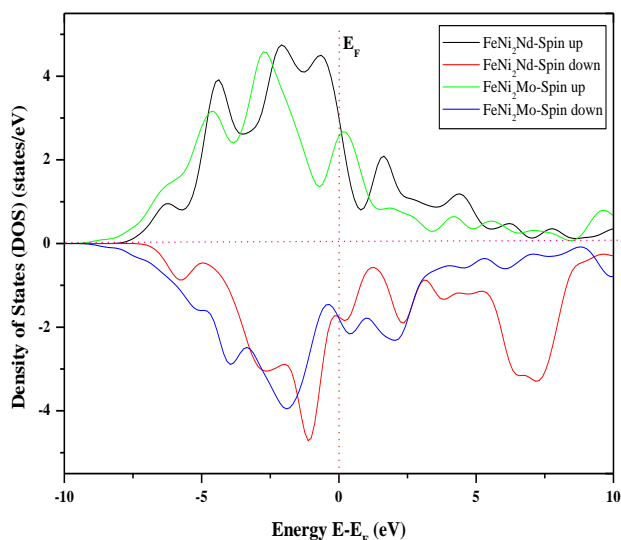


Fig. 4 –Total density of states (TDOS) for:(a) FeNi₂Mo, (b) FeNi₂Nd

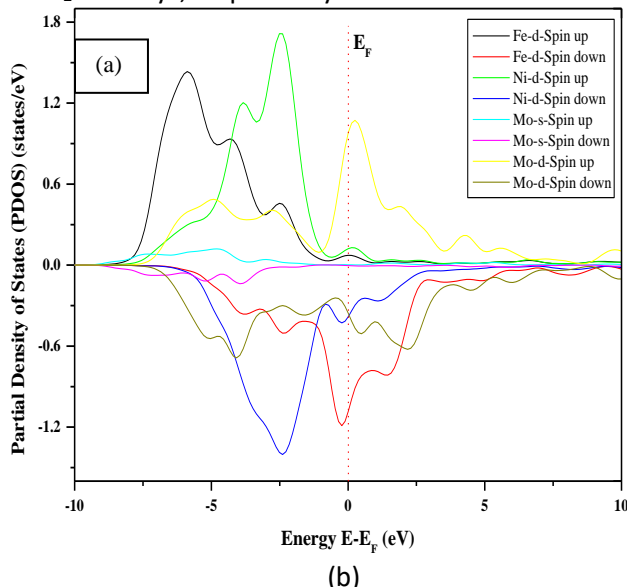
Fig. 4 shows that the calculated TDOS for FeNi₂Mo and FeNi₂Nd alloys has high values with the GGA approximation in the region close to the Fermi level; we find that the TDOS value of FeNi₂Nd is higher than that of FeNi₂Mo, and this indicates that its valence band is rich in electrons. Within the

region close to the fermi level, we note that the highest peak density of states was recorded in FeNi₂Nd alloy, which was estimated at 4.71 (state/eV), while the value 4.63 (state/eV) was recorded as the highest value for FeNi₂Mo. While we find exactly at the fermi level that the largest value for the density of states was recorded at theFeNi₂Nd alloy with a value estimated 2.81 (states/eV).

3.2.3. Partial Density of States (PDOS)

In this work, we have calculated and analyzed the partial density of states (PDOS) of FeNi₂Mo and FeNi₂Nd alloys in order to understand the movement of electrons close to the fermi level. Figs. 5a and 5b show the PDOS of FeNi₂Mo and FeNi₂Nd respectively.

In this paper, we have calculated and analyzed the partial density of states (PDOS) of FeNi₂Mo and FeNi₂Nd alloys in order to understand the movement of electrons close to the Fermi level, where Figs. 5a and 5b show the PDOS of FeNi₂Mo and FeNi₂Nd alloys, respectively.



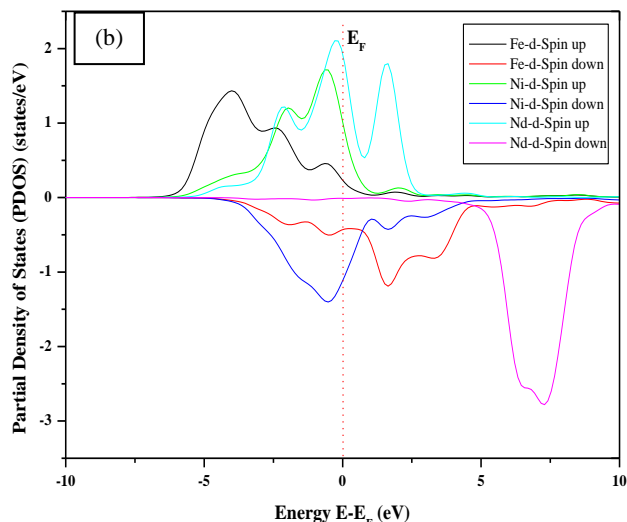


Fig. 5– Partial density of states (PDOS) for: (a) FeNi₂Mo, (b) FeNi₂Nd

In the figure above, we present the density of states on atomic valence orbital (PDOS) in order to compare them with each other and also reveal the role of electrons in different atomic valence orbital, and how they affect the electronic properties. From the different distributions of spin states (spin up and down) represented in the figure, the spin polarization is determined, starting with a single primitive cell and later generalizing to the entire alloys. In order to ascertain more deeply into the contributions of iron and nickel atoms that make up the FeNi₂Mo and FeNi₂Nd alloys, we calculated the expected density of states across electron orbitals as a function of energy ($E-E_F$).

Through the PDOS distributions, shown in Fig. 5a for FeNi₂Mo alloy, it can be shown that the electronic states are mainly located in the active region, which extends from -7 eV to +7 eV around the Fermi levels. To give more detail, near the Fermi level, Ni atoms have larger 3-d-orbital states than the Fe atom; also, the contributions that come from the up-spin Ni 3-d electrons are larger than those from the same down-spin 3-d elements. The 3-d-orbitals contribution of all atoms is also dominant in the electronic distribution of FeNi₂Mo; the same note is made for FeNi₂Nd alloy in Fig. 5b. It is very clear by the two Figures. 5a and 5b that the molybdenum (Mo) or neodymium (Nd) atoms with which the original FeNi₃ alloy was doped have added a lot in the electronic distribution in the region near the Fermi level, and FeNi₂Nd alloy is considered the best

in terms of chemical and catalytic activity from FeNi₂Mo alloy.

3.3. Optical Properties

The study of the optical properties is very important, as its importance lies in obtaining information about the values of the optical constants of the material and its relationship to the photons falling on it. From this information, we can use it to design and manufacture optical blocks and optical pulses using different technologies.

3.3.1. Absorption coefficient

It is defined as the decreasing ratio of the spectrum of incident radiation energies with respect to the unit distance, in the direction of the direction of wave propagation within the material. The absorption coefficient is related to the energy of the incident photons, and from it it is possible to know the nature of the electronic transformations, and its equation is in the form:

$$\alpha = \frac{4\pi K}{\lambda} \quad (1)$$

Where α is absorption coefficient, k is the coefficient of extinction and λ is wave length (cm).

We have calculated the adsorption coefficient value of FeNi₂Mo and FeNi₂Nd alloys with GGA approximation, and they are shown in Fig. 6.

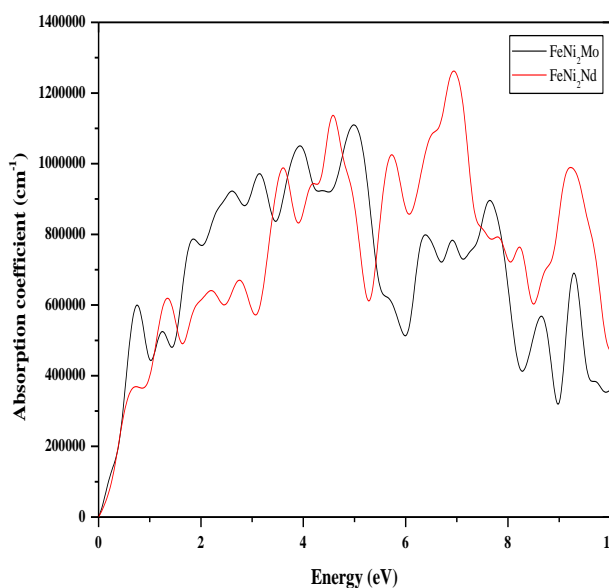


Fig. 6 – Absorption coefficient of FeNi₂Mo and FeNi₂Nd

Fig.6 shows the change in the absorption coefficient as a function of the energy of the incident photon on FeNi₂Mo and FeNi₂Nd alloys. It is clear from the figure that the absorption coefficient in general begins to increase gradually and in an oscillating manner with the increase in the energy of the photons of light, until the energy value 5 eV for the FeNi₂Mo alloy and the value 4.5 eV for FeNi₂Nd alloy, after which the value of the absorption coefficient decreases significantly with the increase in the energy of the incident photons. In general, the behavior of both alloys in absorption is almost the same, except that higher values are recorded sometimes in FeNi₂Nd alloy, this is especially when the amount of energy 6.92 eV with a peak value of 1231000 cm⁻¹. This indicates that the change in the energy of the incident photons leads to different optical behaviors in this material. This result is close to work [25].

3.3.2. Optical Conductivity

It is a physical property that relates the current density to the electric field, and is given by the following equation:

$$\sigma(\omega) = \frac{J(\omega)}{E(\omega)} \quad (2)$$

Where σ is optical conductivity (Sm/m), J is current density (A/m²) and E is electric field (N/C).

The optical conductivity values of FeNi₂Mo and FeNi₂Nd alloys have been calculated with approximations GGA, and the results are written in Fig. 7.

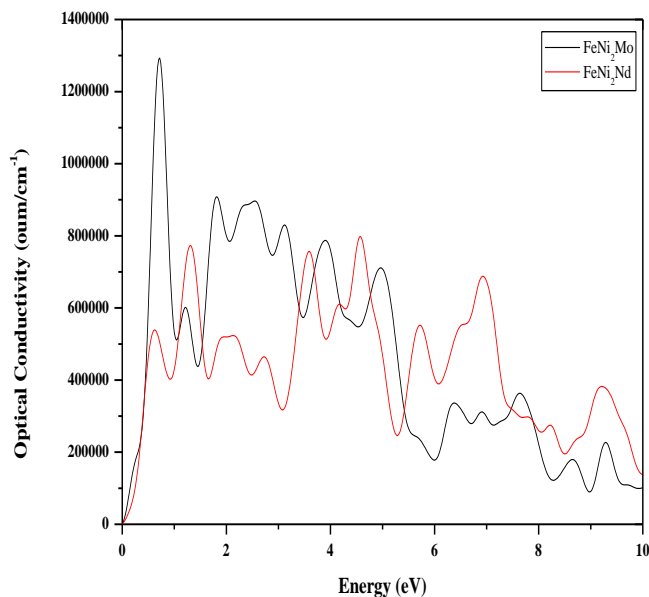


Fig. 7 – Optical conductivity of FeNi₂Mo and FeNi₂Nd

Fig.7 represents the optical conductivity changes in terms of the energy of photons falling on the FeNi₂Mo and FeNi₂Nd alloys using the GGA approximations, in general, we notice that the value of photoconductivity increases with increasing energy of the two alloys, the values fluctuate between increasing at times and decreasing at other times, where we recorded the largest value of photoconductivity in FeNi₂Mo alloy with an estimated value of 1300000 Oum/cm⁻¹, while the highest value of the FeNi₂Nd alloy reached the value 750000oum/cm⁻¹. By comparing the two alloys with each other, FeNi₂Mo alloy appears to be more optically conductive in the infrared and visible ranges. What can be concluded from the analysis of each of the absorption and optical conductivity curves is that FeNi₂Mo alloy has a good absorption value that allows their use in optoelectronics and photovoltaic compounds.

1376

3.3.3. Refractive Index

It is the ratio between the speed of light in free space and its speed in the matter, and the refractive index can be found according to the following equation:

$$n_0 = \left[\left(\frac{1+R}{1-R} \right)^2 - (k_0^2 + 1) \right]^{\frac{1}{2}} + \frac{1+R}{1-R} \quad (3)$$

Where R is reflectivity, K₀ is extinction coefficient.



The refractive index values for FeNi₂Mo and FeNi₂Nd were calculated using the GGA approximations as shown in Fig.8.

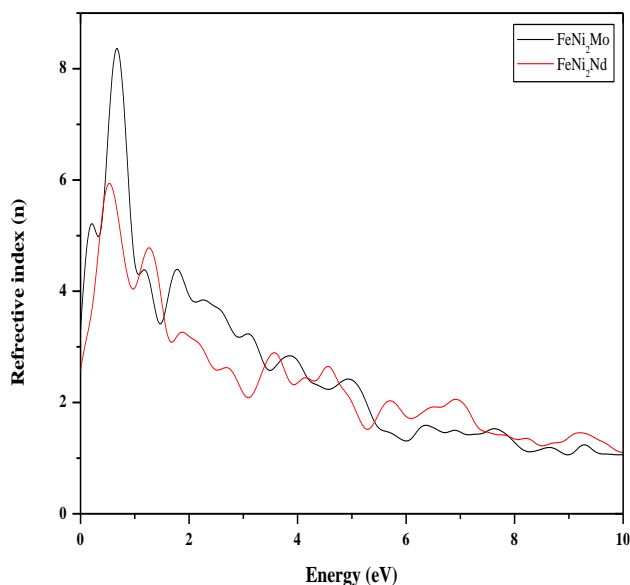


Fig. 8 – Refractive index of FeNi₂Mo and FeNi₂Nd

By Figure 8, which expresses the refractive index in terms of incident photons, we noticed that the refractive index n_0 for the FeNi₂Mo and FeNi₂Nd are 4, 2.84 respectively. Whereas, with the increase in the energy of the incident photons, the value of the refractive index began to increase to reach its maximum value at the energy 1.78 eV and 0.87 eV after that, the values of the refractive index began to decrease sharply, due to the increase in the energy of the incident photons.

4. CONCLUSION

Proceeding from the calculations made according to the density function theory (DFT) and using an approximation, and using the Siesta program, the results obtained for the FeNi₂Mo and FeNi₂Nd alloys, whether structural, electrical or optical, were compared, and the following was concluded:

- There is a clear difference between the structural parameters of the two alloys (FeNi₂Mo and FeNi₂Nd) from the structural parameters of the original alloy (FeNi₃).
- The results of the density of states showed that each of the two alloys has metallic prop-

erties, in addition to that the FeNi₂Nd alloy has a greater magnetic moment

- It was found that the contribution of the 3-d orbital is dominant, and this appears by comparing the density of partial states recorded in the two alloys, and this affects the electronic and magnetic properties of the two alloys.
- The differentiation in the optical properties of the two alloys favors each of them for specific technological uses.

REFERECES

1. Kaur R, Hasan A, Iqbal N, Alam S, Saini M, K, Raza S, K, J. Sep. Sci. 2014; **37**: 1805.
2. Hedayatnasab Z, Abnisa F, Daud W. M. A. W. Mater. Des 2017; **123**: 174.
3. Zaiou S, Beldjebli O, Belfennache D, Tayeb M, Zenikheri F, Harabi, Dig A. J. Nanomater. Biostructures 2023; **18(1)**: 69-82.
4. Zhou K, Zhou X, Liu J, Huang Z. J. Pet. Sci. Eng 2020; **188**: 106943.
5. Jiang B, Lian L, Xing Y, Zhang N, Chen Y, Lu P, Zhang D, Environ. Sci. Pollut. Res 2018; **25**: 30863.
6. Benkrima Y, Belfennache D, Yekhlif R, Soudani M, Souiga, Achour Y. East Eur. J. Phys **2023**; **(2)**: 150-156.
7. Jiang B, Lian L, Xing Y, Zhang N, Chen Y, Lu P, Zhang D. Environ. Sci. Pollut. Res 2018; **25**: 30863.
8. Kongsat P, Kudkaew K, Tangjai J, Edgar A, Pongprayoon T, J. Phys. Chem. Solids 2021; **148**: 109685.
9. Fatima H, Kim K S. Adv. Powder Technol 2018; **29**: 2678.
10. Harada M, Kuwa M, Sato R, Teranishi T, Takahashi M, Maenosono S. ACS Appl. Nano Mater 2020; **3**: 8389.
11. Gloag L, Mehdipour M, Chen D, Tilley R. D., Gooding J. J., Adv. Mater 2019; **31**, 1904385.
12. Jia Z, Kou Z. K, Yin S, Feng A, Zhang C, Liu X, Cao H, Wu G., Compos. Part B Eng 2020; **189**, 107895.
13. Krajewski M, Tokarczyk M, Stefaniuk T, Słomińska H, Małolepszy A, Kowalski G, Lewińska S, Sławska-Waniewska A, Mater. Chem. Phys 2020; **246**: 122812.
14. Wu K.-L., Yu R., Wei X.-W, Cryst. Eng. Comm.



- 2012;**14**; 7626.
15. Achour Y, Benkrima Y, Lefkaier I, Belfenache D, J. Nano- Electron. Phys 2023;**15**: 01018.
 16. Mohamed M.A., El-Maghraby A.H., Abd El-Latif M.M, Farag H.A, Bull. Mater.Sci 2013;**36**: 845.
 17. Yuan Y, Wu H, You M, Li Z, Zhang Y, Surf. Coat.Technol 2019; **378**:124957.
 18. Banl, Drogenik M, Makovec D, J. Magn. Magn.Mater 2006;**307**: 250.
 19. Tanaka A, Yoon S.-H, Mochida I, Carbon 2004;**42**: 1291.
 20. Ordejon P, Artacho E, Soler J.M, Phys. Rev. B. 1996;**53**: R10441.
 21. Hohenberg P, Kohn W, Phys. Rev. B 1964; **136**: 864.
 22. Tuan L, Hoan T. V., Nguyen Duy V, Computational Materials Science 2020;**180**: 109715.
 23. Chen K, Kim S, Rajendiran R, Prabakar K, Li G, Shi Z, Jeong C, Kang J, Li O, Journal of Colloid and Interface Science 2021;**582**: 977.
 24. Hinuma Y, et al., Comput. Mater. Sci 2017; **128**: 140.
 25. Nourozia B, Aminian A, Fili N, Zangeneh Y, Boochani A, Darabi P, Results in Physics 2019;**12**: 2038.

